Characterization of the Solid−Solid Phase Transition of $Co_2(CO)_6(AsPh_3)_2$

Piero Macchi,*,† Luigi Garlaschelli,‡ Secondo Martinengo,‡ and Angelo Sironi*,†

Dipartimento di Chimica Strutturale e Stereochimica Inorganica, Università di Milano e centro CNR CSMTBO, Via G. Venezian 21, 20133 Milano, Italy, and Dipartimento di Chimica Inorganica Metallorganica e Analitica, Università di Milano, Via G. Venezian 21, 20133 Milano, Italy

Received June 24, 1998

The dimeric $Co_2(CO)_6(AsPh_3)_2$ molecule contains an unsupported Co−Co bond, axial arsines, and equatorial carbonyls. At room temperature, the molecule crystallizes in the $R\bar{3}$ space group [$a = 15.473(3)$ Å, $c = 14.240(2)$ Å] packing in chains along *c* which are hexagonally arranged in the **ab** plane. When the temperature is lowered, no significant changes are found in the molecular structure until a second-order phase transition [$T_c = 206(3)$ K] occurs by doubling the *c* axis [at T = 123 K $a = 15.233(4)$ Å, $c = 28.440(6)$ Å, space group $R\bar{3}$]. The major molecular conformational changes related to the phase transition are the rotations of $Co(CO)_3$ and $AsPh_3$ fragments about the 3-fold axes and those of the phenyls about their As−C bond. X-ray studies at 16 different temperatures have been performed in order to describe the details of the small continuous structural changes that occur in the low-temperature phase.

Introduction

As a part of a continuing investigation of the chemistry and stereochemistry of metal (particularly Co and Rh) carbonyl clusters,[1] we studied the substitution reactions of $Co_6(CO)_{16}$ with various ligands. In most cases, degradation of the cluster occurred to give $Co_4(CO)_{12-x}L_x$ species[2] and, with ER_3 (E = P, As), dimeric species as well. In the case of $AsPh_3$, $Co_2(CO)_6(AsPh_3)_2$ (**1**) was obtained as the major product. Because the structure of this compound was assigned only on the basis of IR data, we decided to undertake an X-ray analysis. Further, because of the good quality of the crystals, the high symmetry of this molecule, and the presence of an unsupported Co−Co bond, we thought that this compound was also a good candidate for an accurate low-temperature study of the experimental electron-density distribution,[3] in order to investigate its interesting bonding features. While performing the low-temperature X-ray experiment, we observed at $T = 206(3)$ K a solid−solid reversible phase transition, which is here reported. In the high-temperature (HT) phase, the molecular fragment is centrosymmetric; in the low-temperature (LT) phase, the intramolecular inversion center is lost, the "hexagonal" *c* axis is doubled, the space group remains unchanged.

Experimental Section

Synthesis. **1** was formed in the reaction of $Co_6(CO)_{16}$ with $AsPh_3$ in dichloromethane at room temperature and identified by comparison with an authentic sample prepared according to Manning.[4] The previously unreported IR spectrum in tetrahydrofuran solution shows two bands at 1999(w) and 1980(s) cm^{-1} in the stretching region of the terminal CO's. Because this spectrum is compatible with both D_{3h} and D_{3d} local symmetry of the unbridged $Co_2(CO)_6$ moiety,[5] the staggered D_{3d} conformation of the two sets of radial carbonyl groups was proposed as the more probable on the basis of reduction of steric interactions.[4] Our structural results fully confirm this hypothesis. Crystals suitable for the X-ray analysis were obtained by the slow-diffusion technique: layering cyclohexane over a saturated CH_2Cl_2 solution and leaving the solvents to diffuse; after a few days, several violet crystals (with hexagonal prismatic shape) appeared at the interface between the two phases and were then separated.

Structural Characterization. A crystal of **1** (0.2 × 0.15 × 0.15 mm) was isolated and used for the X-ray analyses. All experiments were carried on a SMART-CCD diffractometer equipped with a nitrogen gas stream LT device (Bruker LT3). In this apparatus, a thermocouple measures the stream temperature inside the nozzle, but the actual temperature on the sample can only be estimated on the basis of the nozzle-to-sample distance. A careful test to estimate the actual temperature on the crystal during variation of the gas flow intensity has been performed using the cell parameters of a test crystal (LRB/081)[6] which was previously collected on a diffractometer equipped with the Samson cryostat. Here, the crystal and the head are in thermal equilibrium at the same temperature which was controlled by a silicon-diode sensor whose accuracy in determining the actual temperature reduces the uncertainty below 1°.

Some general conditions were fixed during the experiments: graphite-monochromatized Mo Kα radiation ($\lambda = 0.710\ 73$ Å); generator at 45 kV and 40 mA; 20 s/frame; detector at 2.94(1) cm from the sample; $(\sin\theta/\lambda)_{max} = 0.85$ Å^{-1}; ω-scan method, $\Delta\omega = 0.3°$.

A preliminary experiment showed the reversibility of the phase transition. Then, data at 16 different temperatures (alternatively below and above T_c) were collected. Three kinds of experiments were performed: (a) at $T = 299$, 224, 218, 208, 199, 184, 170, and 123 K, 1000 frames in two different ϕ settings at negative θ angles were collected (100 additional frames at positive θ were used for correctly estimating the cell parameters); complete sets of unique data (up to

† Dipartimento di Chimica Strutturale e centro CNR CSMTBO.
‡ Dipartimento di Chimica Inorganica.

(1) For instance see: (a) Fumagalli, A.; Martinengo, S.; Bernasconi, G.; Ciani, G.; Proserpio, D. M.; Sironi, A. *J. Am. Chem. Soc.* **1997**, *119*, 1450. (b) Fumagalli, A.; Martinengo, S.; Tasselli, M.; Ciani, G.; Macchi, P.; Sironi, A. *Inorg. Chem.* **1998**, *37*, 2826 and references therein.
(2) (a) Heaton, B. T.; Longhetti, L.; Mingos, D. M. P.; Briant, C. E.; Minshall, P. C.; Theobald, B. R. C.; Garlaschelli, L.; Sartorelli, U. *J. Organomet. Chem.* **1981**, *213*, 333. (b) Darensbourg, D. J.; Incorvia, M. J. *Inorg. Chem.* **1981**, *20*, 1911. (c) Bojczuk, M.; Heaton, B. T.; Johnson, S.; Ghilardi, C. A.; Orlandini, A. *J. Organomet. Chem.* **1988**, *341*, 473.
(3) Macchi, P.; Proserpio, D. M.; Sironi, A., *J. Am. Chem. Soc.*, in press.
(4) Manning, A. R. *J. Chem. Soc. A* **1968**, 1135.
(5) Vohler, O. *Chem. Ber.* **1958**, *91*, 1235.
(6) Destro, R.; Soave, R. *Acta Crystallogr.* **1995**, *C51*, 1383.

10.1021/ic9807240 CCC: $15.00
Published on Web 11/13/1998

Table 1. Cell Parameters, Agreement Indexes (upon refinement), and Total Number of Reflections Collected at Each Temperature

T (K)	a (Å)	c_{HT} or $(c_{LT})/2$ (Å)	V_{HT} or $V_{LT}/2$ (Å^3)	R_1[a]	reflections collected	unique (R_{int}[b])
299	15.473(3)	14.240(2)	2952.5(1.5)	0.0303	10 467	3147 (0.0275)
248	15.409(4)	14.229(3)	2925.5(1.5)	0.0342	2 128	1902 (0.0289)
233	15.392(3)	14.228(2)	2919.2(1.5)	0.0355	1 229	1060 (0.0198)
224	15.391(3)	14.230(2)	2919.2(1.5)	0.0324	6 532	2887 (0.0291)
218	15.385(4)	14.228(2)	2916.6(1.2)	0.0290	8 558	3061 (0.0304)
208	15.375(4)	14.228(2)	2912.8(1.2)	0.0295	12 940	3040 (0.0266)
202[c]	15.359(3)	14.227(5)	2907.0(1.4)	0.0364	4 651	3445 (0.0288)
199[c]	15.353(3)	14.235(3)	2906.1(1.4)	0.0460	15 444	5917 (0.0386)
194[c]	15.347(2)	14.226(2)	2901.6(1.4)	0.0581	2 210	1918 (0.0228)
186[c]	15.334(4)	14.225(4)	2896.7(1.4)	0.0384	9 888	3619 (0.0231)
184[c]	15.333(2)	14.234(9)	2898.0(1.6)	0.0346	19 532	5952 (0.0373)
182[c]	15.329(2)	14.225(4)	2894.7(1.2)	0.0364	2 349	2021 (0.0181)
170[c]	15.318(2)	14.220(4)	2884.6(1.1)	0.0365	15 547	6019 (0.0308)
155[c]	15.282(2)	14.223(4)	2876.7(1.1)	0.0428	5 210	3788 (0.0223)
143[c]	15.267(3)	14.220(2)	2870.4(1.2)	0.0422	1 984	1649 (0.0153)
123[c]	15.233(4)	14.220(6)	2857.6(1.9)	0.0241	14 519	6054 (0.0281)

[a] $R_1 = \Sigma||F_o - F_c||/\Sigma|F_o|$; reflections with $I/\sigma(I) > 2.0$ have been used for refinements. [b] $R_{int} = \Sigma|F_o^2 - F_{mean}^2|/\Sigma F_o^2$; $R_\sigma = \Sigma\sigma(F_o^2)/\Sigma F_o^2$. [c] For these temperatures $c/2$ and $V/2$ are reported.

$\sin\theta/\lambda = 0.7$ Å^{-1}) were available. (b) At $T = 248$, 202, 186, and 155 K, 300 frames (100 at positive θ) were taken, providing ca. 80% of unique data. (c) At $T = 233$, 194, 182, and 143 K, 150 frames (50 at positive θ) were collected, providing ca. 50% of unique data.

Absorption correction was applied to all datasets using SADABS;[7] no crystal decay was observed. A reproducible dependence of cell axes on ω regions was found at each temperature; thus, to have an unbiased picture of the cell dimensions dependence on temperature, cell parameters were obtained upon least-squares fit of integration positioned reflections contained in 150 frames (at positive and negative θ angles) collected in the very same ω-regions at each temperature. A scaling based on five repeated room temperature experiments was applied to standard uncertainties (the uncertainties upon integration are unrealistically small because of the large observations/parameters ratio, and a scale factor of 3.0 was always applied to produce more realistic estimated standard deviation).

Positions of Co and As atoms (both in HT and LT phases) were determined with Patterson methods. All other atoms were located via Fourier difference maps; hydrogens were kept fixed at constant distances from bonded C atoms. A mean C−H distance was finally modeled to 1.08 Å on the basis of an accurate refinement (using Stewart scattering factors for hydrogens) of the extensive LT data.

Anisotropic thermal parameters were assigned to all non-H atoms. Refinements at each temperature were all stable; however, for the type c datasets (only 50% of data) rigid body constraints for phenyl rings were applied. For the data collected very close to T_c, refinements were carried out in both lattices. Results of refinements for each data collection are summarized in Table 1.

Results and Discussion

$Co_2(CO)_6(AsPh_3)_2$ crystallizes in the $R\bar{3}$ space group lying about a $\bar{3}$ symmetry element (b in Wyckoff notation). The molecule contains two trigonal-bipyramidal cobalt atoms linked by an unsupported Co−Co bond along the axial direction (see Figure 1). The two (enantiomeric, i.e., of inverted helicity) $AsPh_3$ ligands are bonded in the remaining axial sites whereas the terminal CO's are equatorially bonded and bent away markedly from the $AsPh_3$ ligands, i.e., toward the opposite Co atom (C−Co−Co ≈ 86°). The observed geometrical features of the $AsPh_3$ fragment fit well into the structural correlation analysis of Ph_3P-X systems:[8] the 3-fold symmetry with Co−As−C−C torsion close to 40° is in the center of the most densely populated zone of the conformational space. The molecules pack in chains along c, and the chains pack hexagonally in the **ab** plane; however, because neighboring chains are shifted (by $c/6$ or $c/3$), the overall packing is trigonal.

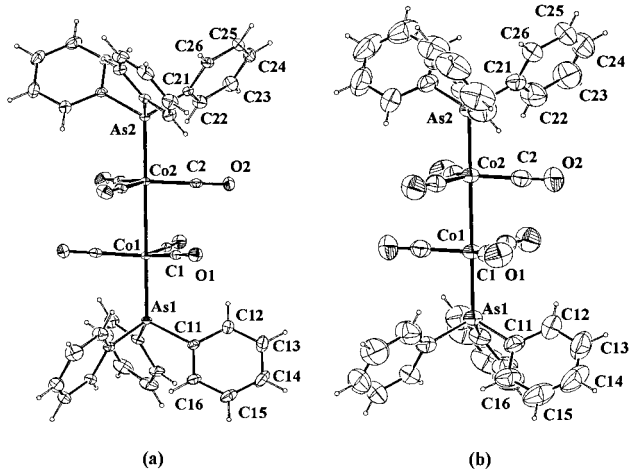

Figure 1. $Co_2(CO)_6(AsPh_3)_2$ molecular structure at (a) $T = 123$ K and (b) room temperature. Ellipsoids of the non-hydrogen atoms are drawn at 50% probability level.

Through examination of the shape of the "enclosure shell" (not shown) of a $Co_2(CO)_6(AsPh_3)_2$ molecule, the packing motif of the crystal is easily decoded into three fundamental components: (a) S_6 "sextuple embraces",[9] which strictly couple the $AsPh_3$ groups of two contiguous molecules along c (see Figure 2); (b) trigonal-helical π stackings, where each phenyl of a $AsPh_3$ group "interacts" with a phenyl of a surrounding chain (see Figure 3); and (c) trigonal gears, arising from phenyl bumps into the (six) holes generated by the staggered conformation of the $Co_2(CO)_6$ moiety, which is somewhat assisted by C−H···O interactions (see Figure 3 and Table 2). All of these features have a gearing character which strongly correlates the movements of the surrounding groups, and this correlation is probably at the heart of the phase transition which is described in the following.

Structural and Conformational Aspects of the Phase Transition. When the temperature is lowered, no significant changes are found in the molecular structure (apart from the expected slight contraction of the interatomic distances)[10] until

(7) Sheldrick, G. M. unpublished work.
(8) Bye, E.; Schweizer, W. B.; Dunitz, J. D. *J. Am. Chem. Soc.* **1982**, *104*, 5893.
(9) Dance, I. In *The Crystal as Supramolecular Entity*; Desiraju, G. R., Ed.; Wiley Chichester, 1995.

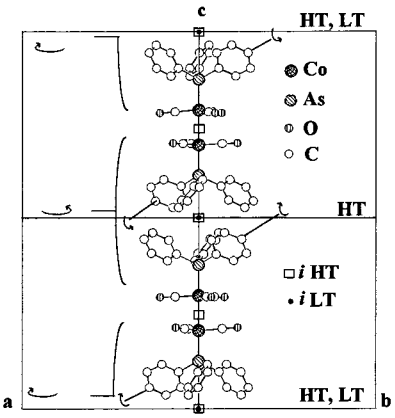

Figure 2. Molecular packing along the *c* axis. The HT phase has an additional intramolecular inversion center (inversion centers are here represented by empty squares for the HT structure and by filled circles for the LT one) which is lost upon phase transition (thus producing the doubling of *c*). The main rotational movements occurring above T_c are also schematically drawn: the opposite rotation of the two "sextuple embraces" about *c* (which involves, to a lesser extent, the carbonyls) and the rotation of phenyl rings about their main librational axis (again preserving the intermolecular inversion center and breaking the intramolecular one) which causes alternated stretching and compressing of the embraces. (For the rotations drawn here, the stretching occurs at the central one.)

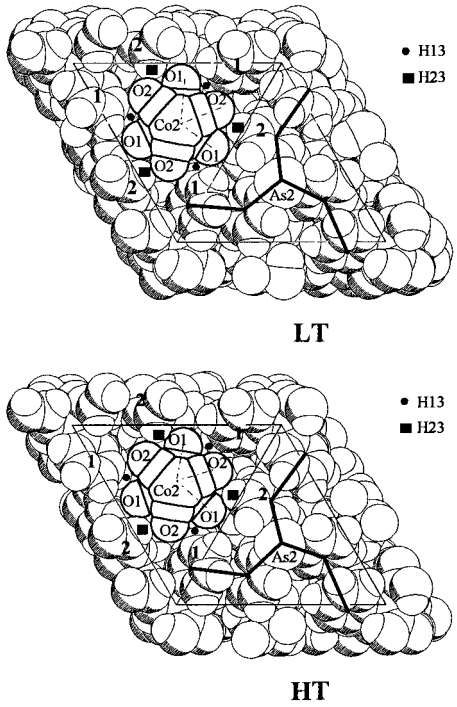

Figure 3. Packing in the **ab** plane. The trigonal-helical π stacking, where each phenyl of a $AsPh_3$ group "interacts" with a phenyl of a surrounding chain, has been outlined by three bold lines. In the HT phase (bottom), the O−Co−Co−O torsions are all 60°; thus, each molecule has six identical holes which host symmetrically the surrounding phenyls. On the other hand in the LT phase (top), the two carbonyl torsions are no longer identical (see Table 2); thus, there are two kinds of holes: phenyl 1 bumps into the larger one while phenyl 2 is somewhat "excluded" from the smaller hole. (Note, however, that $d_{O1-H13} > d_{O2-H23}$.)

T_c is reached. As for the cell parameters, *a* (≡*b*) strongly decreases; but *c* remains substantially unchanged (see Table 1). Below T_c, a number of reflections with half-integer *l* indexes in the HT lattice gain significant intensities. This means that the *c* axis is doubled. In the HT phase, there are two kinds of inversion centers (intra- and intermolecular, respectively; see Figure 2); however, upon refinement of the LT phase structure, it appears that the intramolecular inversion center is lost (thus allowing for the lowering of the molecular symmetry from S_6 to C_3; see Figure 2).[11] Although the lattice has changed its metric, the space group is unchanged, but the molecule now lies about the *c* Wyckoff position. As is usual in solid-state phase transitions, the HT phase is more *symmetric* than the LT phase.

The major conformational changes of the $Co_2(CO)_6(AsPh_3)_2$ molecule, occurring when the temperature is lowered below T_c, are the rotation of the two $Co(CO)_3$ and the two $AsPh_3$ fragments about their 3-fold axes (see the O1−Co1−Co2−O2, C11−As1−As2−C21, and C−As−Co−O torsion angles in Table 2) and the rotation of the phenyls about their As−C bond (which affords different conformations for the two arsines; see Co−As−C−C angles in Table 2). There is also a shift of the whole molecule along *c* which differentiates the two intrachain stackings of the phenyl groups (that were equivalent in the HT phase). The sextuple embrace is strongly sensitive (*only*) to phenyl rotation, as can be derived from the following data: at room temperature, $\phi = 41.7°$, and the As···As distance (*d*) is 7.00 Å, but at 123 K, the two unequivalent embraces have $\phi = 36.8°/d = 7.23$ Å and $\phi = 45.5°/d = 6.76$ Å, respectively. However, because phenyl rotations occur in opposite directions for the two arsines, the *normalized c* axis length (i.e., *c* in the HT phase and *c*/2 in the LT phase) does not change substantially. On the contrary, the packing in the **ab** plane is sensitive to *all* of the above-mentioned changes which can all contribute to a better intermeshing of the chain, but above all, the rotation of the two $Co(CO)_3$ and the two $AsPh_3$ fragments is the key movement which, as it opens three infracarbonyl holes (at the expenses of the other three), allows a denser packing of the chains, hence, the strong shortening of *a* (and *b*).

Determination of T_c and Classification of the Phase Transition. The phase transition has been determined to occur at $T_c = 206(3)$ K on the basis of the following experimental observations:

(a) When the cell volume is plotted against *T* (*V* of the HT phase and *V*/2 of the LT phase), a significant change in its slope is observed (see Figure 4) and the two curves, fitted by linear regression, cross at $T_c = 207$ K. The very same behavior is shown by the *a* axes (Table 1) while *c* has only a small decrease with temperature, and no significant change in its slope (with respect to *c*/2 in the LT phase) can be detected. Because the molar volume does not show discontinuities in the region of the transition, at variance from its first derivative, the transition can be classified as *second order* (according to Ehrenfest's criteria).[12]

(b) As stated above, the loss of the intramolecular inversion center is due mainly to the motion of phenyl and carbonyl groups. The C11−As1−As2−C21 and O1−Co1−Co2−O2 torsion angles are constrained by symmetry to 60° in the HT phase. In the LT phase, instead, torsion angles different from

(10) Atomic distances were corrected for thermal libration according to: Schomaker, V.; Trueblood, K. N. *Acta Crystallogr.* **1968**, *B24*, 63.

(11) Note that two different origin choices can be taken in the $R\bar{3}$space group. In the HT phase, one is centered on the intramolecular inversion center and the other on the intermolecular center. Thus, the doubling of the *c* axes can, in principle, speak for the presence in the unit cell of two centrosymmetric molecules not related by any crystallographic symmetry or two noncentrosymmetric molecules related by an intermolecular inversion center.

(12) Ehrenfest, P. *Proc. Natl. Acad. Sci. U.S.A.* **1933**, *36*, 153.

Table 2. Behavior of Some Relevant Intra- and Intermolecular Bonding Parameters on changing the Temperature[a]

	torsion angles				intermolecular distances	
T (K)	O1−Co1−Co2−O2	C11−As1−As2−C21	C−As−Co−O	Co−As−C−C	O−H5′ (Å)	O−H3 (Å)
299	60.0	60.0	34.2(1)	41.7(2)	2.66	2.48
248	60.0	60.0	33.2(2)	41.7(3)	2.63	2.47
224	60.0	60.0	32.9(1)	41.5(2)	2.63	2.47
218	60.0	60.0	32.9(1)	41.5(2)	2.62	2.47
208	60.0	60.0	33.0(1)	41.5(2)	2.61	2.47
202	60.0(4)	61.0(4)	33.4(2) 32.3(3)	40.8(5) 41.9(5)	2.61 2.61	2.46 2.46
199	60.3(2)	61.2(2)	33.2(2) 32.3(2)	41.1(4) 41.8(4)	2.60 2.60	2.46 2.46
186	62.0(1)	63.9(2)	33.0(2) 31.7(2)	39.8(4) 43.0(4)	2.59 2.60	2.46 2.47
184	62.2(2)	64.6(2)	33.8(1) 31.4(2)	39.6(3) 43.3(2)	2.60 2.60	2.46 2.47
170	63.4(1)	66.9(1)	33.8(1) 30.8(1)	38.5(2) 44.0(2)	2.60 2.60	2.45 2.48
155	64.2(1)	68.3(2)	34.4(2) 30.4(2)	37.9(3) 44.5(3)	2.61 2.60	2.45 2.49
123	65.6(1)	70.8(1)	34.7(1) 29.5(1)	36.8(1) 45.5(1)	2.60 2.58	2.44 2.49

[a] "Long" data collections only. All intermolecular distances reported have uncertainty below 0.01 Å.

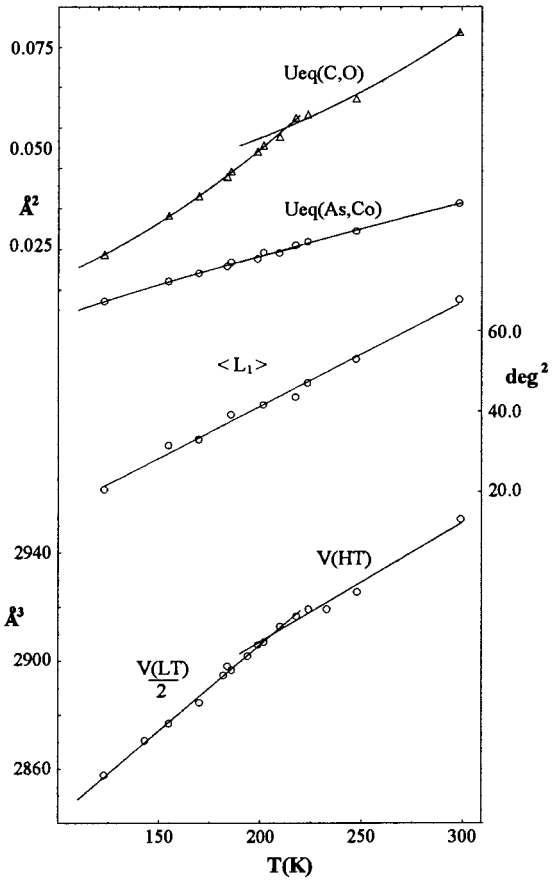

Figure 4. Properties of the crystals plotted as a function of the temperature. On the bottom, the cell volumes of the two phases are reported (note the discontinuous change in the slope that occurs at the transition temperature, which can be estimated by the temperature at which the two linear fittings cross, $T_c = 207$ K). The central plot represents the changes of librations of phenyls about their main librational axis (As−C); the regular and linear dependence on *T* suggests that an order−disorder transition can be safely excluded. On the top, U_{eq} are grouped for heavy (Co, As) and light (C, O) atoms and fitted (linearly and quadratically, respectively) on *T*. Note the abrupt change that occurs for U_{eq} of light atoms at T_c, which might be related to the fact that the heavy atoms are less sensitive to the intermolecular environment which is much more perturbed than the intramolecular one by the phase transition.

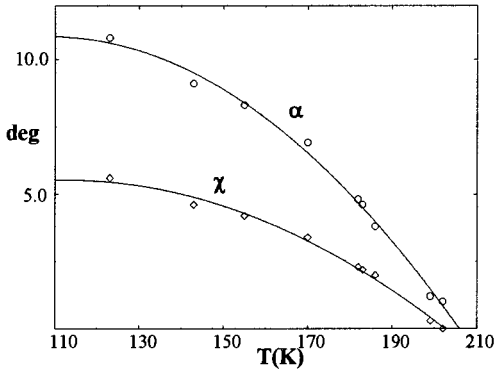

Figure 5. C−As−As−C and O−Co−Co−O torsion angles are fixed to 60° by symmetry in the HT phase (where the molecular symmetry is $\bar{3}$) while they are unconstrained in the LT phase. Here, α (i.e., the angular shift of C−As−As−C from 60°) and χ (that of O−Co−Co−O) are plotted. Through quadratic fitting, $T_c = 206$ and 203 K can be estimated, respectively.

60° are allowed (at $T = 123$ K, they are 70.8° and 65.6°, respectively). The shifts of these two torsions from their HT value (α and χ in Figure 5) are related to the order parameter (η)[13] within the Landau theory[14] of second-order phase transitions, being null by symmetry in the HT phase. Because α and χ change continuously and drop to zero at the critical temperature, the transition is indeed second-order within Landau's criteria (the two phases at T_c are identical). Through the use of a quadratic regression, $T_c = 206$ and 204 K are estimated for α and χ, respectively.

(c) The absolute value of the Co−As−C−C angles must be identical for the two arsines in the HT phase (≈42°, nearly independent from *T*; see Table 2). In the LT phase, instead, the two independent Ph rings have different angles; their difference, $|\phi|$, can be treated as was done before for α and χ and, upon regression, $T_c = 206$ K was obtained.

According to Landau and to the mean-field theory,[14] $\eta \div (T_c - T)^{\beta}$, with $\beta = 0.5$, in phase transitions of minerals, deviations are found only for temperatures very close to T_c.[14c] Here, log/log plots for the selected quantities (α, χ and ϕ) give, by linear regression treatment, an averaged $\beta = 0.73(3)$, which means that there is not a linear dependence between η and α, χ or ϕ.

(d) Reflections with odd *l* indexes in the LT phase are monitored at different temperatures (peak integrations of the HT phases have been performed on the LT lattice as well; thus, the HT forbidden intensities are also available). At $T = 199$ K, 190 of these still have significant intensity[15] (upon merging

(13) Actually, in a displacive phase transition (see the discussion below for the classification of this transition) $\eta = \sum_j u_j$ where u_j is the shift of the *j*th atom from the symmetric HT position.

(14) (a) Landau, L. D.; Lifshitz, E. M. *Statistical Physics*; Addison-Wesley: Reading, MA, 1958. (b) Sirotin, Y. I.; Shakolskaya, M. P. *Fundamentals of Crystal Physics*; Mir Publishers: Moscow, 1982. (c) Dove, M. T. *Am. Mineral.* **1997**, *82*, 213.

and correcting the datasets[16]), but at $T = 208$ K, only 10 reflections have $I/\sigma(I) > 2.0$.[17] Odd *l*-index reflections are on average less intense than even *l*-index ones because the reduction in symmetry is due mainly to phenyls and carbonyls (Co and As still being located on the 3-fold axes and very close to their original position in the HT phase); however, this effect decreases with $\sin\theta/\lambda$ because high-order reflections are more sensitive to small shifts from the lost symmetry, which also affects Co and As, whose contribution to diffraction is overwhelming at high angles.

Additional observations support the phase-transition classification. A differential scanning-calorimetry (DSC) trace did not show an exothermal−endothermal peak in the 173−298 K region but only the sudden change in slope of the curve (centered about 210 K, 25 K wide; scan speed[18] 40° min^{-1}) expected for second-order transformations.[19] The LT group is a translational subgroup of the HT one (HT and LT space groups are identical while the crystal lattice changes, according to $c_{LT} = 2c_{HT}$).

It is also worth noting that, because the point group symmetry $(\bar{3})$ in this phase transformation is preserved, there is only one diffraction domain also in the LT phase, at variance from what happens in transformations without conservation of the crystal point group [for which the loss of one symmetry operation produces *n* kinds of domains (*n* is the multiplicity of the symmetry operator lost)].

At room temperature, the phenyl ring libration about the As−C axis is quite large (ca. 70 deg^2; see Figure 4), and the thermal motion analysis of the $AsPh_3$ as a rigid group shows that a libration about the *c* axis is also present (ca. 20 deg^2). According to the theory of displacive phase transitions,[14c] it is a vibrational (soft) mode, antisymmetric with respect to the symmetry operator lost in the phase transition, that is responsible for the observed atomic displacements. Indeed, the major conformational changes observed in the phase transition can be considered as movements along *some*[20] of the normal modes implied by the above librations. A comparison with the phase transitions observed for poly(phenyls)[19c,21] (order−disorder in *p*-terphenyl, displacive in biphenyl) might be helpful. In general, an order−disorder phase transition implies a multiwell potential surface describing the motion of the HT phase disordered atoms; for *p*-terphenyl, a harmonic double-well model was supported by the reasonable temperature dependence of the librations around the molecular axis for the (two) disordered central rings against the abnormally large, temperature-independent libration (260 deg^2 for *p*-terphenyl at room temperature) "observed" for a single ordered ring.[21d,f,22] Here, a double-well model (and the implied order−disorder phase transition) can be safely excluded on the basis of the "correct" behavior of the phenyl ring librations (which are close to that of an ordered phenyl; see Figure 4) and also on the basis of the continuous change in α, χ and ϕ. In this context, we notice that this libration lacks a sudden change at T_c, while the $\langle U_{eq}\rangle$-(*T*) functions, in particular those of the lightest atoms (C and O), cannot be differentiated at T_c (see Figure 4).

Conclusions

The phase transition reported here can be classified as second-order according to Ehrenfest (because the first derivatives of chemical potential are continuous at T_c) and Landau (because the two phases are identical at T_c), *antiferrodistorsive* (because there is a loss of translational symmetry), *antiferroic*[23] (because there is conservation of the point group symmetry of the crystal), a *type I* Christy's transition[24] (because it shows a group−subgroup relationship between phase symmetries, corresponding to a unique, irreducible representation of the higher symmetry), and *displacive* (because it is caused by only small shifts of atoms from their HT symmetric positions, and an order−disorder mechanism has been proved not to occur).

Solid−solid phase transitions in *molecular crystals* are often considered "unwanted" phenomena,[25] disturbing otherwise simple structural characterizations. Indeed, many of these have been observed by crystallographic methods; however, an accurate characterization (with attempts to determine the transition temperature and the structural changes that occur in the proximity of the transformation) is rare.[26] Here, we have reported on the phenomenology of a second-order phase transition which possibly relates HT phase-active internal motions to the three observed (antisymmetric) deformation paths of the LT phase. From this point of view, we may state that a good reason for studying the structural details of phase transitions is that of adding to the conventional analysis of the anisotropic displacement parameters some information on the correlations between the displacements of the individual atoms which would be otherwise lost.

Acknowledgment. The authors are thankful to Dr. M. Di Pasquantonio (Gruppo di Supporto Analitico Perkin-Elmer) for

(15) Note that at $T = 123$ K, ca. 2000 unique odd *l* reflections have $I/\sigma(I) > 2.0$.

(16) It has been demonstrated that a correction for the nonfiltered $\lambda/2$ intensities has an insignificant effect on the results of structure refinements and accurate ED analysis. See: (a) Kirschbaum, K.; Martin, A.; Pinkerton, A. A. *J. Appl. Crystallogr.* **1997**, *30*, 514. (b) Macchi, P.; Proserpio, D. M.; Sironi, A.; Soave, R.; Destro, R. *J. Appl. Crystallogr.* **1998**, 583. However, $\lambda/2$ contamination has its worst effect in determining the correct cell parameters and space groups (because systematic absences may be violated); thus, a careful correction has been applied to all datasets here.

(17) It is worth noting that some of these forbidden intensities (usually for large θ) are still present even for temperature well above the estimated T_c; besides the difficulties in integrating these very weak and spread reflections ($I/\sigma_{max} = 3.5$), this phenomenon cannot be neglected. The hypothesis of a hysteresis of the LT phase can be safely excluded on the basis of the second-order character of the transition and because they have been also observed at room temperature for a new crystal (before lowering the temperature). It seems to be more reasonable that these intensities are superstructure reflections due to a diffuse scattering originated by long-range correlated motions, which violate the local symmetry.

(18) The nature of a second-order phase transition in a molecular crystal is such that only a high scan speed can enhance the occurrence of the phase transformation in the DSC trace; of course, the usage of such a high rate reduces the instrumental accuracy in the determination of the critical temperature.

(19) (a) Pope, H. I.; Judd, M. D. *Differential Thermal Analysis*; Heyden: London, 1990. (b) Threlfall, F. L. *Analyst* **1995**, *120*, 2435−2460. (c) Cailleau, H.; Baudour, J. L.; Meinnel, J.; Dworkin, A.; Moussa, F.; Zeyen, C. M. E. *Faraday Discuss.* **1980**, *69*, 7.

(20) No phase is conveyed by thermal factors.

(21) (a) Badour, J. L.; Delugeard, Y.; Cailleau, H. *Acta Crystallogr.* **1976**, *B32*, 150. (b) Charbonneau, G. P.; Badour, J. L. *Acta Crystallogr.* **1976**, *B32*, 1420. (c) Charbonneau, G. P.; Delugeard, Y. *Acta Crystallogr.* **1977**, *B33*, 1586. (d) Badour, J. L.; Cailleau, H.; Yelon, W. B. *Acta Crystallogr.* **1977**, *B33*, 1772. (e) Badour, J. L.; Delugeard, Y.; Rivet, P. *Acta Crystallogr.* **1978**, *B34*, 625. (f) Baudour, J. L.; Sanquer, M. *Acta Crystallogr.* **1983**, *B39*, 75. (g) Badour, J. L. *Acta Crystallogr.* **1991**, *B47*, 935.

(22) Brock, C. P.; Schweizer, W. B.; Dunitz, J. D. *J. Am. Chem. Soc.* **1985**, *107*, 6964.

(23) Salje, E. H. K. *Phase Transition in Ferroelastic and Co-Elastic Crystals*; Cambridge University Press: Cambridge, 1993.

(24) (a) Christy, G. A. *Acta Crystallogr.* **1993**, *B49*, 987. (b) Christy, G. A. *Acta Crystallogr.* **1995**, *B51*, 753.

(25) (a) Dunitz, J. D. *Acta Crystallogr.* **1995**, *B51*, 619. (b) Dunitz, J. D.; Bernstein, J. *Acc. Chem. Res.* **1995**, *28*, 193.

(26) For a recent study, see: (a) Destro, R. *Chem. Phys. Lett.* **1997**, *275*, 463 and other work in progress. (b) Dunitz, J. D. *Pure Appl. Chem.* **1991**, *63*, 177. (c) Jagarlapudi, A. R.; Sarma, P.; Dunitz, J. D. *Acta Crystallogr.* **1990**, *B46*, 784. (d) Yang, Q. C.; Richardson, F. R.; Dunitz, J. D. *Acta Crystallogr.* **1989**, *B45*, 312.

the DSC analysis and to Prof. R. Destro for providing a suitable crystal for calibration of the LT device. Prof. N. Masciocchi, Prof. P. Sozzani, Dr. D. M. Proserpio, and Dr. E. Corradi are also thanked.

Supporting Information Available: Tables listing detailed crystallographic data, atomic positional parameters, bond lengths and angles for the room temperature and the $T = 123$ K structures, and DSC trace obtained at 40°/min (12 pages). Ordering information is given on any current masthead page.

IC9807240